




Targeted inactivation of the *Septin2* and *Septin9* genes in myelinating Schwann cells of mice

Ann-Kristin Martens¹ | Michelle Erwig¹ | Julia Patzig¹  | Robert Fledrich¹  | Ernst-Martin Füchtbauer² | Hauke B. Werner¹ 

¹Department of Neurogenetics, Max Planck Institute for Multidisciplinary Sciences, Göttingen, Germany

²Department of Molecular Biology and Genetics, Aarhus University, Aarhus C, Denmark

Correspondence

Hauke B. Werner, Department of Neurogenetics, Max Planck Institute for Multidisciplinary Sciences, Hermann Rein Str. 3, D-37075 Göttingen, Germany, Email: hauke@em.mpg.de

Present address

Robert Fledrich, Institute of Anatomy, University of Leipzig, Leipzig, Germany.

Funding information

Deutsche Forschungsgemeinschaft, Grant/Award Numbers: WE 2720/2-2, WE 2720/4-1, WE 2720/5-1

Abstract

The formation of axon-enwrapping myelin sheaths by oligodendrocytes in the central nervous system involves the assembly of a scaffolding septin filament comprised of the subunits SEPTIN2, SEPTIN4, SEPTIN7 and SEPTIN8. Conversely, in the peripheral nervous system (PNS), myelin is synthesized by a different cell type termed Schwann cells, and it remained unknown if septins also assemble as a multimer in PNS myelin. According to prior proteome analysis, PNS myelin comprises the subunits SEPTIN2, SEPTIN7, SEPTIN8, SEPTIN9, and SEPTIN11, which localize to the paranodal and abaxonal myelin subcompartments. Here, we use the *Cre/loxP*-system to delete the *Septin9*-gene specifically in Schwann cells, causing a markedly reduced abundance of SEPTIN9 in sciatic nerves, implying that Schwann cells are the main cell type expressing SEPTIN9 in the nerve. However, *Septin9*-deficiency in Schwann cells did not affect the abundance or localization of other septin subunits. In contrast, when deleting the *Septin2*-gene in Schwann cells the abundance of all relevant septin subunits was markedly reduced, including SEPTIN9. Notably, we did not find evidence that deleting *Septin2* or *Septin9* in Schwann cells impairs myelin biogenesis, nerve conduction velocity or motor/sensory capabilities, at least at the assessed timepoints. Our data thus show that SEPTIN2 but not SEPTIN9 is required for the formation or stabilization of a septin multimer in PNS myelin *in vivo*; however, its functional relevance remains to be established.

KEYWORDS

Charcot–Marie–Tooth (CMT) disease, hereditary neuralgic amyotrophy (HNA), myelin outfoldings, myelin sheath, Schwann cell, Septin 2, Septin 9, tomaculae

1 | INTRODUCTION

Rapid impulse propagation along vertebrate axons is achieved by their electrical insulation with myelin. Myelin sheaths restrict action potentials to short unmyelinated axonal segments, the nodes of Ranvier,

thereby accelerating nerve conduction velocity (NCV) 20- to 100-fold (Hartline & Colman, 2007). Thus, myelination enables normal motor, sensory, and cognitive capabilities.

Comprised of multiple concentric, compacted layers of specialized plasma membrane, myelin is synthesized by oligodendrocytes in the central nervous system (CNS) and Schwann cells in the peripheral nervous system (PNS). The ultrastructure of axon/myelin-profiles appears almost similar when comparing CNS and PNS with respect to the

Ann-Kristin Martens and Michelle Erwig contributed equally to this study and should be considered joint first author.

This is an open access article under the terms of the [Creative Commons Attribution-NonCommercial](https://creativecommons.org/licenses/by-nc/4.0/) License, which permits use, distribution and reproduction in any medium, provided the original work is properly cited and is not used for commercial purposes.

© 2022 The Authors. *Cytoskeleton* published by Wiley Periodicals LLC.

predominant compact myelin subcompartment, as well as of non-compact subcompartments including paranodal myelin (adjacent to the nodes of Ranvier) and adaxonal myelin (innermost layer). However, oligodendrocytes and Schwann cells are distinct cell types with marked differences in developmental origin, molecular profiles, and cellular anatomy (Nave & Werner, 2021). For example, peripheral myelin comprises characteristic non-compacted channels through compact myelin termed Schmidt-Lanterman incisures (SLI), which provide a cytosolic connection between the abaxonal and the adaxonal myelin layer (Nave & Werner, 2014; Terada et al., 2019). Additionally, CNS and PNS myelin display distinct—though overlapping—protein compositions. This is exemplified by myelin protein zero (MPZ/P0), an Ig-like adhesion protein constituting a dominant 44% of the total PNS myelin protein (Siems et al., 2020) but absent from CNS myelin (Möbius, Patzig, Nave, & Werner, 2008; Yin et al., 2006; Yoshida & Colman, 1996). Indeed, MPZ/P0 is required for the compaction of PNS myelin (Giese, Martini, Lemke, Soriano, & Schachner, 1992; Martini, Mohajeri, Kasper, Giese, & Schachner, 1995; Patzig et al., 2016), reflecting that a different set of structural proteins establishes the normal ultrastructure and function of myelin in the CNS and the PNS.

Septins are small GTP-binding proteins that can multimerize and form higher-order structures, many of which associate with the cytoplasmic surfaces of plasma membranes of a broad range of species and cell types (Hamdan et al., 2020; Shuman & Momany, 2021; Woods & Gladfelter, 2021). A septin filament comprised of the subunits SEPTIN2, SEPTIN4, SEPTIN7, and SEPTIN8 localizes to and scaffolds the adaxonal myelin layer in the CNS, thereby preventing pathological outfoldings of entire myelin sheaths (Patzig et al., 2016). Experimental mice lacking this filament display a slowing of CNS NCV by about 20% (Erwig et al., 2019; Patzig, Erwig, et al., 2016) in the absence of other recognizable neuropathology, suggesting that myelin outfoldings caused by septin deficiency per se can impair the speed of impulse propagation. Importantly, myelin outfoldings are a frequent neuropathological phenomenon in both the CNS (Bowley, Cabral, Rosene, & Peters, 2010; Cullen & Webster, 1979; Djannatian et al., 2021; Erwig et al., 2019; Hill, Li, & Grutzendler, 2018; Katanov et al., 2020; Patzig, Erwig, et al., 2016; Snaidero et al., 2014; Sturrock, 1976) and the PNS (Adlkofer et al., 1995; Bolino et al., 2004; Fabrizi et al., 2000; Gillespie et al., 2000; Goebbels et al., 2012; Golan et al., 2013; Horn et al., 2012; Stendel et al., 2007), in which they represent a hallmark of tomaculous neuropathies.

Here, we ask if—in similarity to CNS myelin—septin subunits also assemble as multimers in PNS myelin, and, if so, if their deficiency is associated with myelin outfoldings and reduced NCV. Individual septin subunits have been previously observed in PNS myelin, mainly by immunolabeling of teased fiber preparations. To the best of our knowledge, the first septin subunit reported in PNS myelin was SEPTIN7 in SLI, paranodal, and abaxonal PNS myelin (Roth, Ivanova, & Colman, 2006). Subsequently, SEPTIN9 was found expressed in Schwann cells (Sudo et al., 2007), SEPTIN2 was identified as enriched in paranodal myelin (Ogawa & Rasband, 2009), SEPTIN2, SEPTIN7, SEPTIN8, SEPTIN9, and SEPTIN11 were found localizing to SLI, paranodal, and abaxonal PNS myelin (Buser, Erne, Werner, Nave, &

Schaeren-Wiemers, 2009), and several of these subunits were reported to be expressed throughout PNS myelination (Patzig et al., 2011; Roth, Liazoghli, Perez De Arce, & Colman, 2013). The presence of SEPTIN9 in non-compact abaxonal PNS myelin was also confirmed by immuno-electron microscopy on cryo-sectioned sciatic nerves (Patzig et al., 2011). A more recent comprehensive proteomic assessment of all proteins comprised by PNS myelin showed that only SEPTIN2, SEPTIN7, SEPTIN8, SEPTIN9, and SEPTIN11—but no other septin subunits—display considerable abundance in PNS myelin (Siems et al., 2020). The 13 mammalian septins are categorized as four groups according to their homology; subunits within one group may substitute for each other in a multimer (Kinoshita, 2003). Canonically, six or eight subunits of three or four septin groups interact with each other, thereby forming hexamers or octamers as the core of the assembly of higher order structures (Cavini et al., 2021; Woods & Gladfelter, 2021). It is thus noteworthy that PNS myelin comprises septin subunits from all four homology groups, that is, the SEPT2-group (SEPTIN2), SEPT3-group (SEPTIN9), SEPT6-group (SEPTIN8, SEPTIN11), and SEPT7-group (SEPTIN7).

Our work provides evidence that, indeed, a septin multimer consisting of SEPTIN2, SEPTIN7, SEPTIN8, SEPTIN9, and SEPTIN11 exists in PNS myelin. Notably, SEPTIN2 but not SEPTIN9 is required for its formation or stabilization. At the same time, *Septin2* mutant mice lacking a PNS myelin septin multimer provide an optimal negative control for localization studies on teased fiber preparations, which confirm the previously reported localization to SLI, paranodal, and abaxonal PNS myelin. However, in difference to mice lacking CNS myelin septins (Erwig et al., 2019; Patzig, Erwig, et al., 2016), we do not find evidence of impaired myelin formation or slowed NCV in mice lacking a PNS myelin septin multimer. This indicates that septin multimers display different subunit compositions and functions for the structure and function of myelin in the CNS and the PNS.

2 | MATERIALS AND METHODS

2.1 | Animal welfare

All animal experiments were performed in accordance with the German animal protection law (TierSchG) and approved by the Niedersächsisches Landesamt für Verbraucherschutz und Lebensmittelsicherheit (LAVES) under license 33.19-42502-04-15/1850. All procedures were supervised by the animal welfare officer for the Max Planck Institute of Multidisciplinary Sciences (MPI-NAT), Göttingen, Germany. The animal facility at the MPI-NAT is registered according to §11 Abs. 1 TierSchG.

2.2 | Mouse models

Embryonic stem cells (ES) harboring an engineered allele of the *Septin2* gene (*Sept2^{tm1a(EUCOMM)Wtsi}* allele) was acquired from the European Conditional Mouse Mutagenesis Program (Eucomm,

Munich, Germany). ES were microinjected into blastocysts derived from FVB mice, and embryos were transferred to pseudo-pregnant foster mothers, yielding chimeric males. For ES clone EPD0175-4-D03, germ line transmission was achieved upon breeding with C57BL/6 N-females. The lacZ/neo cassette was excised in vivo upon interbreeding with mice expressing FLIP recombinase (129S4/SvJae-Sor-Gt(ROSA)26Sortm1(FLP1)Dym/J; backcrossed into C57BL/6 N), yielding mice carrying a *Sept2^{fllox}* allele (also referred to as *Sept2^{tm1c}*; for scheme see Figure 1c). To inactivate expression of *Septin2* in Schwann cells, exon 5 was excised in vivo upon appropriate interbreedings of *Sept2^{fllox}* mice with mice expressing Cre (see below). Routine genotyping of the *Sept2* allele was by genomic PCR using sense primer P1 (5'-GAAGGCGCTA GAGATTGAACC; binding 5' of the 5' loxP-site) in combination with antisense primers P2 (5'-GGCAGCATGC TAGAAGGAGAG; binding the segment flanked by loxP-sites) and P4 (5'-GAGCAACCTG TCCTCTGGCTG; binding 3' of the 3'loxP site). The *Sept2^{fllox}* allele was detected using primers P1 and P2, yielding a 704 bp product. The recombined allele was detected using primers P1 and P4, yielding a 388 bp product. The wild-type allele was detected by primers P1 and P2, yielding a 511 bp product.

Transgenic *Dhh^{Cre}* mice were previously published (Jaegle et al., 2003). All experiments involving *Dhh^{Cre}* were performed with mice in which the transgene was either present heterozygously or absent. *Cnp^{Cre}* knock-in mice were previously published (Lappe-Siefke et al., 2003). All experiments involving *Cnp^{Cre}* were performed with mice in which the *Cnp^{Cre}* allele was either present heterozygously or absent. *Sept9^{fllox}* mice (also referred to as *Sept9^{TM2-EMFLU}*) were previously published (Füchtbauer et al., 2011). All experiments were performed with mice harboring either the *Sept9^{fllox}* or the *Sept2^{fllox}* allele homozygously, that is, *Sept9^{fllox/fllox}* mice and *Sept2^{fllox/fllox}* mice served as controls. Genotypes were determined by genomic PCR as described. Mutant mice were analyzed together with littermate controls as far as possible. All experiments and analyses were performed blinded to the genotype. Age of experimental mice is given in the figure legends. Mice were bred and kept in the mouse facility of the MPI-NAT.

2.3 | Immunoblotting

Immunoblotting was performed on sciatic nerve lysates as described (Patzig, Kusch, et al., 2016; Schardt et al., 2009). Briefly, mice were sacrificed by cervical dislocation. Sciatic nerves were dissected and homogenized in RIPA buffer with protease inhibitor (50 mM Tris/Cl pH 7.5, 150 mM NaCl, 1 mM EDTA, 1% Triton X-100, 0.5% sodium deoxycholate; Roche complete protease inhibitor) using the Peqlab precelly homogenizer. After 15 min on ice, probes were centrifuged and supernatant was stored at -80°C . Protein abundance was determined using the DC Protein Assay (Biorad). Antibodies were specific for SEPTIN2 (ProteinTech Group; 1:500); SEPTIN7 (IBL; 1:5,000); SEPTIN8 (ProteinTech Group; 1:1,000); SEPTIN9 (ProteinTech Group; 1:1,000); SEPTIN11 (Huang et al., 2008; 1:5,000); actin (Milipore; 1:5,000); myelin-associated glycoprotein (MAG) (Clone 513; Covance;

1:500); cyclic nucleotide phosphodiesterase (CNP; Sigma; 1:1,000); PO/MPZ (Archelos et al., 1993; 1:5,000); and PMP22 (Sigma, 1:1,000), HRP-coupled secondary antibodies were from dianova. Immunoblots were scanned using the Intas ChemoCam system.

2.4 | Teased fiber preparations and immunolabeling

Teased fiber preparations of sciatic nerves and immunolabeling were performed as described (Eichel et al., 2020; Patzig, Kusch, et al., 2016). Briefly, for teased fiber preparations, sciatic nerves dissected from mice of the indicated genotypes at 8–10 weeks of age were transferred into ice-cold PBS and processed. Using two fine forceps (Dumont No. 5), the epineurium was removed and small nerve pieces were transferred onto a new coverslip. By carefully pulling apart the fiber bundles with both forceps, axons were separated from each other. Slides were dried and stored at -20°C . For immunolabeling, teased fiber preparations were consecutively incubated in 4% PFA for 5 min, 100% methanol for 5 min, 3×5 min PBS and 1 hr blocking buffer (PBS, 10% horse serum and 0.1% Tween-20) at RT. Primary antibodies were applied in blocking buffer overnight at 4°C . Samples were washed in PBS 3×5 min. Secondary antibodies diluted in blocking buffer were applied for 1 hr at RT and afterward samples were washed with PBS 3×5 min and 2×30 s in ddH₂O before mounting using Aqua-Poly/Mount (Polysciences, Eppenheim, Germany). Antibodies were specific for MAG (clone 513; Chemicon; 1:50); SEPTIN2 (Huang et al., 2008; 1:50); SEPTIN7 (IBL; 1:1,000); SEPTIN8 (Protein Tech Group; 1:1,000); and SEPTIN9 (Protein Tech Group; 1:1,000). Secondary antibodies were donkey a-rabbit-Alexa488 (Invitrogen, 1:1,000); donkey a-rat-Alexa488 (Invitrogen, 1:2,000); goat a-mouse Cy3 (Dianova, 1:1,000); and donkey a-mouse Alexa555 (Invitrogen, 1:1,000). Images were obtained by confocal microscopy (Leica SP5). Signal was collected with the objectives HCX PL APO lambda blue63.0 3 1.20 WATER UV or HCX PL APO CS 63.0 31.30 GLYC 218C UV. An argon laser with the excitation of 488 nm was used to excite the Alexa488 fluorophore, and the emission was set to 500–573 nm. The laser DPSS 561 was used to excite the Cy3 or Alexa555 fluorophores, and the emission was set to 573–630 nm. DAPI was excited with 405 nm and collected between 417 and 480 nm. LAS AF lite and Fiji were used to export the images as tif files. All conditions and microscope settings were identical when analyzing control and mutants to allow for the direct comparability of fluorescence intensities.

2.5 | Nerve morphology

Light microscopy was performed as described (De Monasterio-Schrader et al., 2013; Patzig, Kusch, et al., 2016). Briefly, mice were anesthetized with Avertin and trans-cardially perfused with HBSS followed by 2% glutaraldehyde and 4% PFA in phosphate buffer containing 0.5% NaCl. Sciatic nerves dissected from perfused mice were

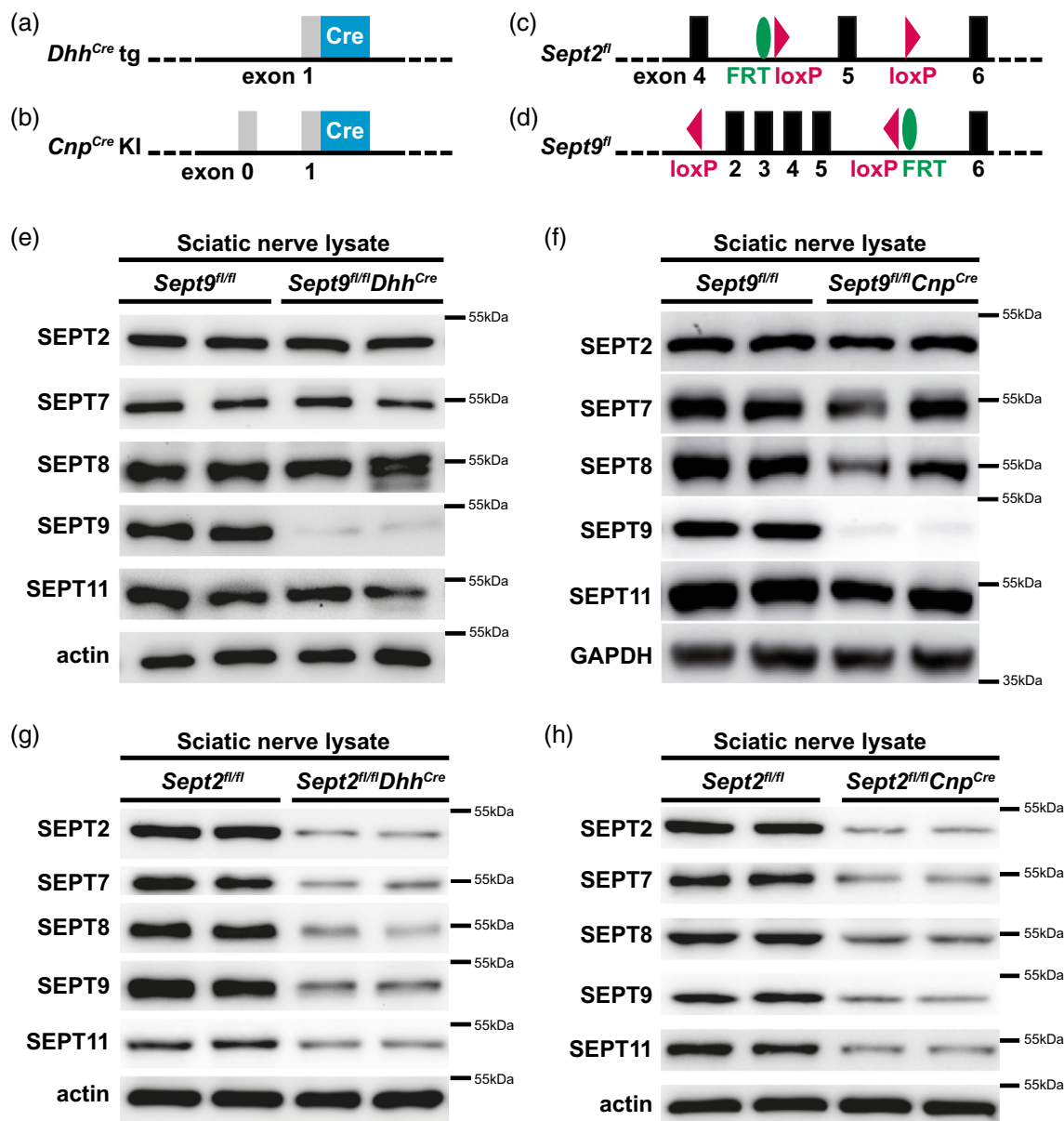


FIGURE 1 Immunoblot analysis of septins when Schwann cells lack *Septin2* or *Septin9*. (a–d) Schemes showing genetic changes in mouse lines used in this work. Positions of the Cre open-reading frame, FRT, and loxP sites are indicated. Schemes not to scale. (a) Transgenic line expressing Cre recombinase in the Schwann cell lineage under control of the *Dhh*-gene promoter (Jaegle et al., 2003). (b) Knock-in line expressing Cre in both Schwann cells and oligodendrocytes under control of the *Cnp*-gene promoter (Lappe-Siefke et al., 2003). (c) Floxed allele of the *Septin2*-gene (*Sept2^{fl/fl}*). (d) Floxed allele of the *Septin9*-gene (*Sept9^{fl/fl}*) (Füchtbauer et al., 2011). (e–h) Immunoblots of sciatic nerve lysates of mice dissected at postnatal Day 75 (P75) comparing the abundance of the septin subunits SEPTIN2, SEPTIN7, SEPTIN8, SEPTIN9, and SEPTIN11 between the indicated genotypes. Blots show $n = 2$ mice per genotype; the same amount of protein was loaded when comparing genotypes. Actin or GAPDH were detected as controls. (e) Comparing *Sept9^{fl/fl}*; *Dhh^{Cre}* with *Sept9^{fl/fl}* mice by immunoblot indicates that the small (39 kDa) isoform of SEPTIN9 is expressed in sciatic nerves of *Sept9^{fl/fl}* control mice but markedly reduced in abundance in *Sept9^{fl/fl}*; *Dhh^{Cre}* mice. Note that other septin subunits display equal abundance between genotypes. (f) By immunoblot, the small (39 kDa) isoform of SEPTIN9 is readily detected in sciatic nerves of *Sept9^{fl/fl}* control mice but markedly reduced in abundance in *Sept9^{fl/fl}*; *Cnp^{Cre}* mice. Other septin subunits display equal abundance between genotypes. (g) Immunoblotting indicates that all assessed septin subunits are expressed in sciatic nerves of *Sept2^{fl/fl}* control mice but markedly reduced in abundance in *Sept2^{fl/fl}*; *Dhh^{Cre}* mice. (h) By immunoblot, all assessed septin subunits are readily detected in sciatic nerves of *Sept2^{fl/fl}* control mice but markedly reduced in abundance in *Sept2^{fl/fl}*; *Cnp^{Cre}* mice.

postfixed in 1% OsO₄ in 0.1 M sucrose and embedded in epoxy resin (Serva). Semithin sections were examined by light microscopy at $\times 100$ magnification using a bright-field light microscope (Zeiss Axio

Imager Z1) coupled to a Zeiss AxioCam MRc camera controlled by Zeiss ZEN 1.0 software. Analysis was performed on one section per mouse and $n = 3$ –4 mice per genotype using ImageJ. The nerve area

was measured by outlining the outer border of the nerve and measuring the area. Images of nerve sections were superimposed with a grid of 2,500 μm^2 sized squares (>70 grids per nerve). For calculating the total number of myelinated axons per nerve or area, the number of myelinated axons was counted in 10 squares distributed across the nerve and not adjacent to each other and then calculated for the nerve or area. The same squares were assessed to count axon/myelin units with myelin outfoldings and to calculate the percentage of axon/myelin units.

2.6 | NCV measurement

Standard electroneurography was performed on mice of indicated genotypes at indicated ages using a Toennies Neuroscreen (Jaeger, Hoechberg, Germany) as previously described (Fledrich et al., 2019). Briefly, mice were anesthetized with intraperitoneal injection of ketamine hydrochloride/xylazine hydrochloride (100 mg kg^{-1} BW/mg kg^{-1} BW). A pair of steel needle electrodes (Schuler Medizintechnik, Freiburg, Germany) was placed subcutaneously along the nerve at sciatic notch (proximal stimulation). A second pair of electrodes was placed along the tibial nerve above the ankle (distal stimulation). Supramaximal square wave pulses lasting 100 ms were delivered using a Toennies Neuroscreen (Jaeger). Compound muscle action potential (CMAP) was recorded from the intrinsic foot muscles using steel electrodes. Both amplitudes and latencies of CMAP were determined. The distance between the two sites of stimulation was measured alongside the skin surface with fully extended legs and NCVs were calculated automatically from sciatic nerve latency measurements. Sensory nerve conduction measurement was performed at the tail; a pair of steel needle recording electrodes was placed upright at the tail base (5 mm apart at the tail sides avoiding blood strangulation) followed by two proximal stimulation electrodes exactly 50 mm distally. The ground electrode was placed subcutaneously between the pairs. Increasing current pulses were delivered until supramaximal stimulation was achieved and the compound action potential reached a plateau. Sensory nerve compound action potential and sensory nerve potential latencies were measured and used to calculate the sensory NCV (sNCV).

2.7 | Plantar test

The plantar test was performed using Dynamic Plantar Aesthesiometer 37450 (Ugo Basile). In the test, the touch stimulator, a metal stick, is placed under the paw and presses on the paw with increasing pressure until the plantar reflex is elicited and the paw is lifted. The latency is measured. Each mouse was subjected to the test three times for the left and three times for the right hind paw within 1 day. For analysis, values from left and right hind paws were combined and the minimal, mean and maximal retraction latencies were taken. In Figure 3m,n, the maximal response time is given.

2.8 | Rotarod assay

Motor performance was measured using the RotaRod system (Technical Services for Electronics [TSE]) with RotaRod TSE V4.0.9 software as reported (Werner et al., 2013). The test measures the time before a mouse falls from a rotating cylinder (rod) while increasing the speed over time. The time spent on the cylinder is given as the latency to fall. Mice were placed on the roller at rest. After 15 s, the starting speed was set to 5 rpm, increasing in regular intervals to 60 rpm within 2 min. In a series of trials per animal, the latency to fall off was measured. Each mouse was tested on two consecutive days as plotted in Figure 3o,p.

2.9 | Statistics

Statistical analysis and compilation of graphs was carried out in GraphPad Prism 9. Graphs plot mean \pm SEM as error bars. Data points represent biological replicates, except for the RotaRod data (Figure 3o,p) in which data points represent the mean. Statistical tests are given in the figure legends. Unpaired two-tailed t test was applied, except for the RotaRod (Figure 3o,p) for which two-way analysis of variance was performed. A p -value $<.05$ was considered the threshold for significance. p -Values are given in the figures.

3 | RESULTS

To delete the *Septin9* gene in Schwann cells, we interbred mice harboring a floxed allele (herein termed *Sept9^{fllox}*, also referred to as *Sept9^{TM2-EMFU}*; Figure 1d) (Füchtbauer et al., 2011) with transgenic mice in which Cre recombinase is expressed in the Schwann cell lineage under control of the desert hedgehog (*Dhh*) gene promoter (Figure 1a) (Jaegle et al., 2003) or with knock-in mice expressing Cre in myelin-forming Schwann cells and oligodendrocytes under control of the cyclic nucleotide phosphodiesterase (*Cnp*) gene promoter (Figure 1b) (Lappe-Siefke et al., 2003). By immunoblotting, the small 39 kDa splice isoform of SEPTIN9 was readily detectable in sciatic nerve lysates of *Sept9^{fl/fl}* control mice (Figure 1e,f). Importantly, its abundance was markedly reduced in lysates of sciatic nerves dissected from both *Sept9^{fl/fl};Dhh^{Cre}* (Figure 1e) and *Sept9^{fl/fl};Cnp^{Cre}* (Figure 1f) mice. However, when using immunoblot to compare the abundance of the other septin subunits expressed in PNS myelin, SEPTIN2, SEPTIN7, SEPTIN8 and SEPTIN11 were detected at similar abundance in sciatic nerve lysates of *Sept9* mutants and control mice (Figure 1e,f). This confirms that SEPTIN9 is robustly expressed in Schwann cells and implies that Schwann cells are the major cell type expressing SEPTIN9 in sciatic nerves.

We then hypothesized that deleting the expression of another septin subunit in Schwann cells may affect the abundance of other septins subunits additional to the septin genetically targeted. We selected the *Septin2* gene for targeting considering that SEPTIN2 is the only septin group III member identified in PNS myelin (Siems

et al., 2020). We thus generated mice harboring a floxed allele (herein termed *Sept2^{fllox}*, also referred to as *Sept2^{tm1c}*; Figure 1c), which we interbred with *Dhh^{Cre}* and *Cnp^{Cre}* mice. Indeed, by immunoblotting the abundance of SEPTIN2 was strongly reduced in lysates of sciatic nerves dissected from both *Sept2^{fl/fl};Dhh^{Cre}* (Figure 1g) and *Sept2^{fl/fl};Cnp^{Cre}* (Figure 1h) mice compared to respective *Sept2^{fl/fl}* control mice (Figure 1g,h). Importantly, by immunoblotting the abundance of SEPTIN7, SEPTIN8, SEPTIN9, and SEPTIN11 was also considerably reduced in sciatic nerve lysates of *Sept2* mutants compared to control mice (Figure 1g,h). Considering that both *Dhh^{Cre}* and *Cnp^{Cre}* mice are suited to recombine floxed target genes specifically in Schwann cells, this confirms that SEPTIN2, SEPTIN7, SEPTIN8, SEPTIN9, and SEPTIN11 are expressed in Schwann cells. Additionally it shows that expression of SEPTIN2 is required to establish or maintain the abundance of all these septin subunits in sciatic nerves.

We note that recombination of the *Septin2* and *Septin9* genes mediated by Cre as expressed in *Dhh^{Cre}* and *Cnp^{Cre}* mice led to effectively similar results in these experiments. For all further experiments (Figures 2 and 3), we focused on using *Dhh^{Cre}* mediated recombination because *Cnp^{Cre}* (but not *Dhh^{Cre}*) recombines target genes not only in Schwann cells but also in oligodendrocytes, which may create difficulties in interpreting some experimental readouts.

We then turned to teased fiber preparations of sciatic nerves because they allow immunolabeling proteins of interest in individual axon/myelin units. In particular, the method allows to determine a protein's localization in myelin subcompartments, that is, in compact myelin versus the non-compact myelin compartments (SLI, paranodal, adaxonal, and abaxonal myelin). In these experiments, MAG serves as marker mainly localizing to SLI, adaxonal and paranodal myelin. Conversely, the abundance of MAG is lower in the abaxonal myelin subcompartment; compact myelin is not immunolabeled by MAG. We found that immunolabeling of SEPTIN2, SEPTIN7, SEPTIN8, and SEPTIN9 in control mice was in agreement with a localization in paranodal myelin (Figure 2a,g,m,s) and abaxonal myelin including the abaxonal part of the SLI (Figure 2d,j,p,v). When immunolabeling teased fibers dissected from *Sept9^{fl/fl};Dhh^{Cre}* mice, SEPTIN9 was virtually undetectable (Figure 2t,w) while SEPTIN2, SEPTIN7 and SEPTIN8 did not display visibly altered localization (Figure 2b,e,h,k,n,q). Importantly, when immunolabeling teased fibers dissected from *Sept2^{fl/fl};Dhh^{Cre}* mice, not only SEPTIN2 (Figure 2c,f) but also SEPTIN7, SEPTIN8, and SEPTIN9 were virtually undetectable (Figure 2i,l,o,r,u,x). In agreement with the immunoblots (Figure 1e,f), these findings show that expression of SEPTIN2—but not of SEPTIN9—in Schwann cells is required to establish or maintain the abundance of other septin subunits expressed in PNS myelin.

To assess if myelin biogenesis is impaired when Schwann cells lack *Septin9* or *Septin2*, we dissected sciatic nerves from *Sept9^{fl/fl};Dhh^{Cre}* mice, *Sept2^{fl/fl};Dhh^{Cre}* mice and respective control mice. By quantitative assessment of semithin cross sections (Figure 3a–d), we found that the number of normal-appearing myelinated axons was similar when comparing *Sept9^{fl/fl};Dhh^{Cre}* with *Sept9^{fl/fl}* mice (Figure 3c) or *Sept2^{fl/fl};Dhh^{Cre}* with *Sept2^{fl/fl}* mice (Figure 3d). Signs of axonal degeneration were not observed and not quantified. Myelin profiles

ensheathing more than one axon or Remak bundles comprising large-caliber axons were not observed; if present these would indicate a radial sorting defect, a common impairment of Schwann cell development in many neuropathy models (Feltri, Poitelon, & Previtali, 2016; Previtali, 2021). Considering that the most evident morphological consequence for CNS myelin of deleting septin expression in oligodendrocytes is the formation of pathological myelin outfoldings (Erwig et al., 2019; Patzig, Erwig, et al., 2016), we quantified myelin outfoldings in the sciatic nerves of *Sept9^{fl/fl};Dhh^{Cre}* mice, *Sept2^{fl/fl};Dhh^{Cre}* mice and respective control mice (Figure 3e,f). However, the number of myelin outfoldings was unchanged. Together, we found no morphological evidence for impaired biogenesis of PNS myelin when Schwann cells lack *Septin9* or *Septin2*.

For the analysis of myelin proteins by immunoblot, we assessed total sciatic nerve lysates for the abundance of two markers for non-compact myelin (MAG, CNP) and two markers for compact myelin (PO/MPZ, PMP22). As expected, these myelin proteins were readily detected in nerves dissected from *Sept9^{fl/fl}* and *Sept2^{fl/fl}* control mice (Figure 3g,h). Importantly, none of the tested myelin proteins differed visibly in abundance in nerves dissected from *Sept9^{fl/fl};Dhh^{Cre}* mice or *Sept2^{fl/fl};Dhh^{Cre}* mice, respectively. Together, except for myelin septins (Figure 1e–h), we found no evident molecular changes in the abundance of PNS myelin proteins when Schwann cells lack *Septin9* or *Septin2*.

We then assessed if deficiency of *Septin9* or *Septin2* in Schwann cells alters NCV by measuring motor NCV (mNCV) in the sciatic nerves (Figure 3i,j) and sensory NCV (sNCV) in the tail nerve (Figure 3k,l). However, we observed no differences when comparing *Sept9^{fl/fl};Dhh^{Cre}* with *Sept9^{fl/fl}* mice (Figure 3i,k). When comparing *Sept2^{fl/fl};Dhh^{Cre}* with *Sept2^{fl/fl}* mice (Figure 3j,l), both mNCV and sNCV displayed a trend toward slower conduction that however did not reach significance. Finally, we tested behavioral capabilities by measuring the latency to retrieve a paw upon a mechanical stimulus (plantar test; Figure 3m,n) and the latency to fall from an accelerating rod (rotarod; Figure 3o,p). However, no differences were observed when comparing *Sept9^{fl/fl};Dhh^{Cre}* with *Sept9^{fl/fl}* mice (Figure 3m,o) or *Sept2^{fl/fl};Dhh^{Cre}* with *Sept2^{fl/fl}* mice (Figure 3n,p). Together, these assessments did not reveal evidence for markedly impaired morphology or functions of peripheral nerves when Schwann cells lack expression of *Septin9* or *Septin2*.

4 | DISCUSSION

Here, we used the Cre/loxP system to recombine floxed alleles of the *Septin2* and *Septin9* genes specifically in Schwann cells, the myelin-forming cells of the PNS. According to proteome analysis (Siems et al., 2020), SEPTIN2 and SEPTIN9 are the only members of their respective homology groups present in PNS myelin of mice (Table 1), implying that other septin subunits are unlikely to compensate for their deficiency (Kinoshita, 2003). Upon deletion of the *Septin9* gene, the abundance of SEPTIN9-protein was strongly diminished in a major peripheral nerve, the sciatic nerve. This indicates that Schwann cells

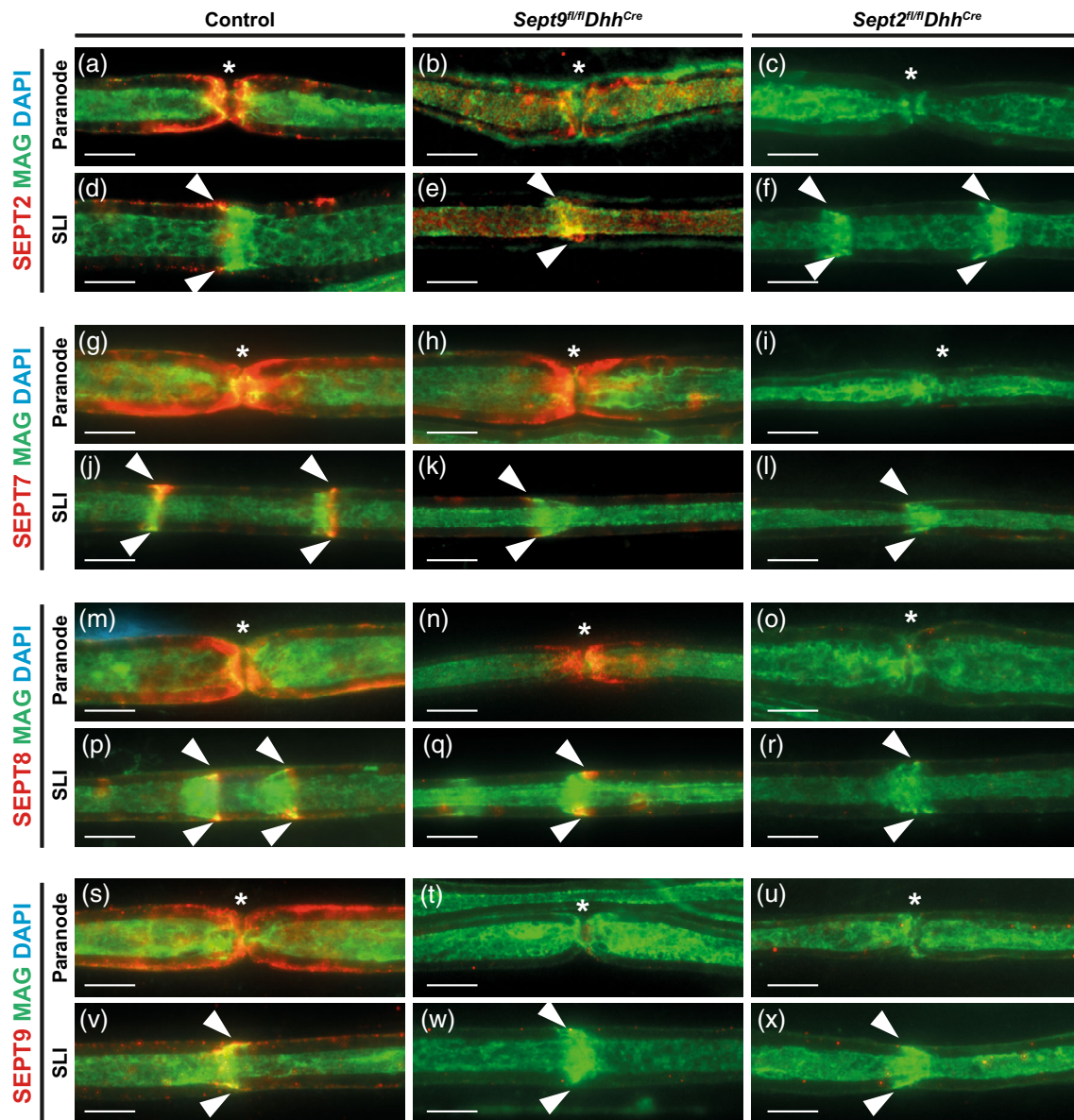


FIGURE 2 Teased fiber analysis of septins when Schwann cells lack *Septin2* or *Septin9*. Confocal microscopic analysis of immunolabeled teased fiber preparations of sciatic nerves of mice dissected at 9–10 weeks of age comparing the septin subunits SEPTIN2, SEPTIN7, SEPTIN8, and SEPTIN9 (in red) between the indicated genotypes. Myelin associated glycoprotein (MAG) (in green) was detected as marker for non-compact myelin, that is, mainly Schmidt-Lanterman incisures (SLI), adaxonal and paranodal myelin. The abaxonal myelin compartment is also immunopositive for MAG, though less intensely. SEPTIN2, SEPTIN7, SEPTIN8, and SEPTIN9 are readily detected at both paranodes (a, g, m, s) and SLI (d, j, p, v) of control mice. SEPTIN2, SEPTIN7 and SEPTIN8 immunolabeling was readily detected in nerves dissected from *Sept9^{fl/fl};Dhh^{Cre}* mice (b, e, h, k, n, q) whereas SEPTIN9 was virtually undetectable (t, w). SEPTIN2, SEPTIN7, SEPTIN8, and SEPTIN9 immunolabeling was essentially undetectable in nerves dissected from *Sept2^{fl/fl};Dhh^{Cre}* mice (c, f, i, l, o, r, u, x). Images show $n = 1$ mouse per genotype representative of $n = 3$ mice per genotype. Stars indicate nodes; arrowheads point at SLI. Scale bars 10 μm .

are the main cell type expressing SEPTIN9 in this nerve. It was interesting that the small 39 kDa isoform of SEPTIN9 was the main isoform detected in control nerves, while larger isoforms that comprise additional N-terminal domains (Connolly et al., 2014; McIlhatton et al., 2001) were virtually undetectable. In difference to *Septin9* mutants, upon deletion of the *Septin2* gene all septin subunits expressed in PNS myelin were strongly diminished additional to

SEPTIN2 itself, that is, SEPTIN7, SEPTIN8, SEPTIN9, and SEPTIN11. It is likely that these subunits are degraded if not stabilized by their incorporation into a PNS myelin septin multimer (Estey, Di Ciano-Oliveira, Froese, Bejide, & Trimble, 2010; Kinoshita, Field, Coughlin, Straight, & Mitchison, 2002; Sellin, Sandblad, Stenmark, & Gullberg, 2011; Tooley et al., 2009), which requires SEPTIN2. Our data thus imply that expression of SEPTIN2—but not of SEPTIN9—is

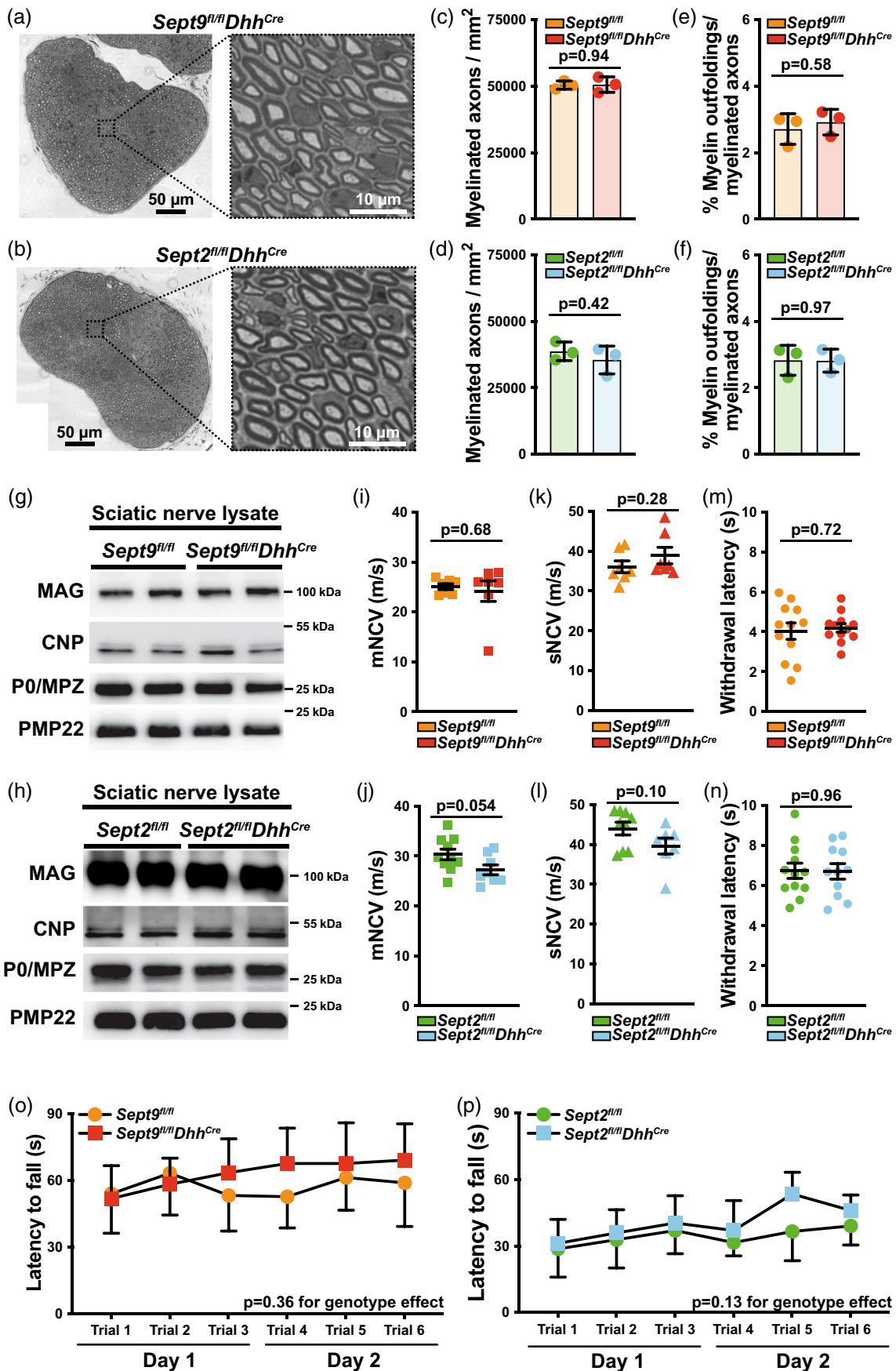


FIGURE 3 Legend on next page.

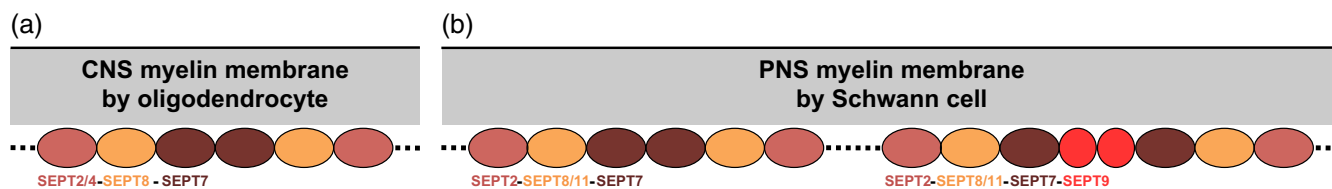


FIGURE 4 Hypothetical model of septin multimers in central nervous system (CNS) and peripheral nervous system (PNS) myelin. Scheme showing septin multimers in CNS myelin (a) and PNS myelin (b) based on the presence of septin subunits according to myelin proteome analysis and the current view of the assembly of septin multimers from subunits. Subunits belonging to the same septin group are depicted in the same color.

essential for the assembly of a septin multimer in Schwann cells. This observation is in agreement with the view that SEPTIN9 (or other SEPT3-group members) may enhance the formation of octamers, but that hexamers can also form without SEPT3-group members (Cavini et al., 2021; Woods & Gladfelter, 2021). Indeed, mammalian septin complexes were observed as hexamers composed of subunits from the SEPT2, SEPT6, and SEPT7-groups, while octamers additionally contain SEPTIN9 or other SEPT3-group members (Kim, Froese, Estey, & Trimble, 2011; Sellin et al., 2011; Sellin, Stenmark, & Gullberg, 2014). Considering the current view on the organization of septin monomers within core multimers (DeRose et al., 2020; Iv et al., 2021; Mendonça et al., 2019; Soroor et al., 2021), it is likely that both, octameric SEPTIN 2-8/11-7-9-9-7-8/11-2 and hexameric SEPTIN 2-8/11-7-7-8/11-2 core oligomers can assemble in Schwann cells, and that hexameric SEPTIN 2-8/11-7-7-8/11-2 oligomers still form when Schwann cells lack SEPTIN9 (Figure 4).

Myelin outfoldings are a frequently observed neuropathology in both the CNS and the PNS. We have previously reported myelin outfoldings and reduced NCV in the CNS when CNS myelin lacks a septin filament due to deletion of *Septin8* or *Anln* in oligodendrocytes (Erwig et al., 2019; Patzig, Erwig, et al., 2016). Conversely, the present work did not reveal evidence of myelin outfoldings or overly slowed nerve conduction in the PNS when PNS myelin lacks a septin multimer upon

deletion of *Septin2* in Schwann cells. We note that we cannot exclude that peripheral nerves may display impairment at earlier or later time-points than those assessed here. We can also not exclude that the non-significant trend toward slowed NCV observed in *Sept2^{fl/fl};Dhh^{Cre}* mice may be more pronounced and possibly significant in larger species that have longer nerves than mice. Yet the present data imply that myelin septins—when comparing CNS and PNS (Table 1)—not only display different subunit compositions and localization to different myelin subcompartments, but also different functional relevance. Notably, oligodendrocytes and Schwann cells differ with respect to their cellular anatomy and molecular profiles (Nave & Werner, 2021), including structural myelin proteins. For example, myelin basic protein (MBP) is essential for myelination in the CNS because its basic charges bind to and thereby cover the negatively charged headgroups of membrane lipids, allowing close proximity of the adjacent cytoplasmic surfaces of myelin membranes during developmental myelin compaction (Musse, Gao, Homchaudhuri, Boggs, & Harauz, 2008; Nawaz et al., 2009; Nawaz, Schweitzer, Jahn, & Werner, 2013). Considering that this function is commonly considered crucial for myelination, it has been surprising that MBP-deficient shiverer mice display only moderate hypomyelination in the PNS (Mikoshiba, Kohsaka, Takamatsu, & Tsukada, 1981; Peterson & Bray, 1984). During myelination in the PNS, however, the function of MBP can be compensated for by

FIGURE 3 Absence of evidence for severe impairments in peripheral nerves of mice lacking *Septin2* or *Septin9* from Schwann cells. Analysis of sciatic nerve morphology, myelin proteins, nerve conduction velocity (NCV) and motor/sensory capabilities of *Sept9^{fl/fl};Dhh^{Cre}*, *Sept2^{fl/fl};Dhh^{Cre}* and respective control mice. (a–f) Light micrographs (a, b) and genotype-dependent quantification (c–f) of semithin-sectioned sciatic nerves dissected at P14 from the indicated genotypes shows a similar number of normal-appearing myelinated axons (c, d) and myelin outfoldings (e, f) when comparing *Sept9^{fl/fl};Dhh^{Cre}* with *Sept9^{fl/fl}* mice (c, e) or *Sept2^{fl/fl};Dhh^{Cre}* with *Sept2^{fl/fl}* mice (d, f). Scale bar sizes are given (in a, b). $n = 3$ per genotype; not significant ($p > .05$) by unpaired two-tailed t test; p -values are given (in c–f). (g, h) Immunoblot analysis of sciatic nerves dissected at P75 shows similar abundance of myelin proteins (MAG, CNP, PO/MPZ, PMP22) when comparing *Sept9^{fl/fl};Dhh^{Cre}* with *Sept9^{fl/fl}* mice (g) or *Sept2^{fl/fl};Dhh^{Cre}* with *Sept2^{fl/fl}* mice (h). Blots show $n = 2$ mice per genotype. The same amount of protein was loaded when comparing genotypes. (i–l) Electrophysiological assessment of motor nerve conduction velocity (mNCV in i, j) measured on both sciatic nerves of each mouse and averaged, as well as of sensory nerve conduction velocity (sNCV in k, l) measured on the tail nerve of each mouse comparing *Sept9^{fl/fl};Dhh^{Cre}* with *Sept9^{fl/fl}* mice at 6 months of age (i, k) as well as *Sept2^{fl/fl};Dhh^{Cre}* with *Sept2^{fl/fl}* mice (j, l) at 1 year of age. $n = 7$ –10 mice per genotype; not significant ($p > .05$) by unpaired two-tailed t test; p -values are given (in i–l). (m, n) The latency of retracting a hind-paw upon a mechanical stimulus (plantar test) was compared between *Sept9^{fl/fl};Dhh^{Cre}* and *Sept9^{fl/fl}* mice at P45 (m) as well as between *Sept2^{fl/fl};Dhh^{Cre}* and *Sept2^{fl/fl}* mice at 32 weeks of age (n). $n = 11$ –12 mice per genotype; not significant ($p > .05$) by unpaired two-tailed t test; p -values are given (in m, n). (o, p) The latency of falling from an accelerating rotating rod was compared between *Sept9^{fl/fl};Dhh^{Cre}* and *Sept9^{fl/fl}* mice at 2.5 months of age (o) as well as between *Sept2^{fl/fl};Dhh^{Cre}* and *Sept2^{fl/fl}* mice at 6 months of age (p). Several trials were performed on two consecutive days. $n = 5$ –8 mice per genotype; not significant ($p > .05$) for an effect of genotype by two-way analysis of variance (ANOVA); p -values for the effect of genotype are given (in o, p).

TABLE 1 Comparison of myelin septins in the CNS and the PNS. Selected features of myelin septins are listed according to analysis of mice. Key references are given

Cell type	CNS myelin	PNS myelin
	Oligodendrocytes	Schwann cells
Septin subunits in myelin ^a		
Group I (SEPT9-group)	SEPTIN9 (very low abundant)	SEPTIN9 (38 kDa isoform)
Group II (SEPT6-group)	SEPTIN8	SEPTIN8, SEPTIN11
Group III (SEPT2-group)	SEPTIN2, SEPTIN4	SEPTIN2
Group IV (SEPT7-group)	SEPTIN7	SEPTIN7
Reference (myelin proteome)	Jahn et al. (2020)	Siems et al. (2020)
Predicted core septin multimer	2/4-8-7-7-8-2/4	2-8/11-7-(9-9)-7-8/11-2
Septin localization in myelin	Adaxonal	Abaxonal, paranodal
Essential for multimer in vivo	<i>Septin8</i>	<i>Septin2</i>
Consequence of deletion in mice	Myelin outfoldings, reduced NCV	Normal-appearing myelin, normal NCV
Reference (mouse mutant)	Patzig, Erwig, et al. (2016)	This work

Abbreviations: CNS, central nervous system; NCV, nerve conduction velocity; PNS, peripheral nervous system.

^aSeptin homology groups according to Kinoshita (2003).

the cytoplasmic domain of the unrelated MPZ/PO (Martini et al., 1995; Martini & Schachner, 1997), and possibly by the lipid-associated peripheral myelin protein 2 (PMP2) (Suresh, Wang, Naneekar, Kursula, & Edwardson, 2010). In this respect, it is relevant to note that we cannot formally exclude that unidentified other molecules may compensate for the deficiency of PNS myelin septins when Schwann cells lack *Septin2* or *Septin9*.

In humans, point mutations or partial duplication of the *Septin9* gene can cause two types of peripheral neuropathy, hereditary neuralgic amyotrophy (HNA) (Collie et al., 2010; Hannibal et al., 2009; Kuhlenbäumer et al., 2005; Laccione et al., 2008; Landsverk et al., 2009; Neubauer et al., 2019) or Charcot-Marie-Tooth disease (CMT) (Grosse, Bauer, Kopp, Schrader, & Osmanovic, 2020). It is of note that the diseases show autosomal-dominant inheritance, and, to the best of our knowledge, no disease-causing *null*-mutations have been identified by now. Indeed, mutant SEPTIN9 variants display altered interactions with other septin subunits and microtubules at least in vitro (Sudo et al., 2007; Bai et al., 2013), suggesting a gain-of-function pathomechanism. However, disease-causing point mutations may also enhance the translation of *Septin9*-transcripts (McDade, Hall, & Russell, 2007), suggesting that not only point mutations but also increased abundance of SEPTIN9 may affect the assembly or stability of septin multimers (Kim et al., 2011), including in PNS myelin. In possible similarity, a gene dosage effect owing to the duplication of the *PMP22* gene encoding peripheral myelin protein of 22 kDa (PMP22) is the most common cause of the most frequent neuropathy, CMT type 1A (Pantera, Shy, & Svaren, 2020). Together, the cell type-specific *null*-mutant mice analyzed here are probably not suited as genuine models for HNA or CMT. We speculate that introducing point mutations or duplications into the rodent genome may allow scrutinizing the suggested gain-of-function pathomechanism in vivo and provide the prerequisite for testing rational therapy approaches.

5 | CONCLUSION

A septin multimer composed of the subunits SEPTIN2, SEPTIN7, SEPTIN8, SEPTIN9, and SEPTIN11 exists in the non-compact paranodal and abaxonal compartments of PNS myelin; SEPTIN2—but not SEPTIN9—is essential for its formation or stabilization. We did not find evidence that PNS myelin septins are required for normal radial sorting or myelination of peripheral axons or for nerve conduction in the PNS. Importantly, this is in difference to the septin filament in the adaxonal compartment of CNS myelin composed of SEPTIN2, SEPTIN4, SEPTIN7, and SEPTIN8, which is required for preventing myelin outfoldings and for normal nerve conduction in the CNS. These results support the concept that oligodendrocytes and Schwann cells utilize different but overlapping sets of structural proteins to facilitate the normal morphology and function of their myelin sheaths.

ACKNOWLEDGMENTS

The authors thank R. Jung for technical support, the European Conditional Mouse Mutagenesis Program (Eucomm) for ES cells harboring the *Sept2*-tm1a allele, U. Bode for culturing ES cells, the transgene facility of the MPI-NAT for blastocyst injections, the electron microscopy facility headed by W. Möbius for support, W. Trimble and J. Archelos-Garcia for antibodies, and K.-A. Nave for support made possible by a European Research Council Advanced Grant (“MyelinNano” to KAN). This work was funded by German Research Foundation (DFG) grant WE 2720/2-2 to H. B. W. Funding was also provided by DFG grants WE 2720/4-1 and WE 2720/5-1 to H. B. W. The funders had no role in study design, data collection and interpretation, or the decision to submit the work for publication. Open Access funding enabled and organized by Projekt DEAL.

CONFLICT OF INTEREST

The authors declare no conflict of interest.

DATA AVAILABILITY STATEMENT

All relevant data are included in this article.

ETHICS STATEMENT

All animal experiments were performed in accordance with the German animal protection law (TierSchG) and approved by the Niedersächsisches Landesamt für Verbraucherschutz und Lebensmittelsicherheit (LAVES) under license 33.19-42502-04-15/1850. All procedures were supervised by the animal welfare officer for the Max Planck Institute of Multidisciplinary Sciences, Göttingen, Germany. The animal facility at the Max Planck Institute of Multidisciplinary Sciences is registered according to §11 Abs. 1 TierSchG.

ORCID

Julia Patzig  <https://orcid.org/0000-0001-5976-9592>

Robert Fledrich  <https://orcid.org/0000-0001-5323-7958>

Hauke B. Werner  <https://orcid.org/0000-0002-7710-5738>

REFERENCES

- Adlkofer, K., Martini, R., Aguzzi, A., Zielasek, J., Toyka, K. V., & Suter, U. (1995). Hypermylelination and demyelinating peripheral neuropathy in Pmp22-deficient mice. *Nature Genetics*, *11*, 274–280.
- Archelos, J. J., Roggenbuck, K., Scheider-Schaulies, J., Linington, C., Toyka, K. V., & Hartung, H.-P. (1993). Production and characterization of monoclonal antibodies to the extracellular domain of PO. *Journal of Neuroscience Research*, *35*, 46–53.
- Bai, X., Bowen, J. R., Knox, T. K., Zhou, K., Pendziwiat, M., Kuhlenbäumer, G., ... Spiliotis, E. T. (2013). Novel septin 9 repeat motifs altered in neuralgic amyotrophy bind and bundle microtubules. *Journal of Cell Biology*, *203*(6), 895–905.
- Bolino, A., Bolis, A., Previtali, S. C., Dina, G., Bussini, S., Dati, G., ... Wrabetz, L. (2004). Disruption of Mtmr2 produces CMT4B1-like neuropathy with myelin outfolding and impaired spermatogenesis. *Journal of Cell Biology*, *167*, 711–721.
- Bowley, M. P., Cabral, H., Rosene, D. L., & Peters, A. (2010). Age changes in myelinated nerve fibers of the cingulate bundle and corpus callosum in the rhesus monkey. *Journal of Comparative Neurology*, *518*, 3046–3064.
- Buser, A. M., Erne, B., Werner, H. B., Nave, K.-A., & Schaeren-Wiemers, N. (2009). The septin cytoskeleton in myelinating glia. *Molecular and Cellular Neuroscience*, *40*, 156–166.
- Cavini, I. A., Leonardo, D. A., Rosa, H. V. D., Castro, D. K. S. V., D'Muniz Pereira, H., Valadares, N. F., ... Garratt, R. C. (2021). The structural biology of septins and their filaments: An update. *Frontiers in Cell and Development Biology*, *9*, 765085.
- Collie, A. M. B., Landsverk, M. L., Ruzzo, E., Mefford, H. C., Buysse, K., Adkins, J. R., ... Hannibal, M. C. (2010). Non-recurrent SEPT9 duplications cause hereditary neuralgic amyotrophy. *Journal of Medical Genetics*, *47*, 601–607.
- Connolly, D., Hoang, H. G., Adler, E., Tazearslan, C., Simmons, N., Bernard, V. V., ... Montagna, C. (2014). Septin 9 amplification and isoform-specific expression in peritumoral and tumor breast tissue. *Biological Chemistry*, *395*, 157–167.
- Cullen, M. J., & Webster, H. D. (1979). Remodelling of optic nerve myelin sheaths and axons during metamorphosis in *Xenopus laevis*. *Journal of Comparative Neurology*, *184*, 353–362.
- De Monasterio-Schrader, P., Patzig, J., Möbius, W., Barrette, B., Wagner, T. L., Kusch, K., ... Werner, H. B. (2013). Uncoupling of neuroinflammation from axonal degeneration in mice lacking the myelin protein tetraspanin-2. *Glia*, *61*, 1832–1847.
- DeRose, B. T., Kelley, R. S., Ravi, R., Kokona, B., Beld, J., Spiliotis, E. T., & Padrick, S. B. (2020). Production and analysis of a mammalian septin hetero-octamer complex. *Cytoskeleton*, *77*, 485–499.
- Djannatian, M., Weikert, U., Safaiyan, S., Wrede, C., Kislinger, G., Ruhwedel, T., ... Simons, M. (2021). Myelin biogenesis is associated with pathological ultrastructure that is resolved by microglia during development. *bioRxiv*.
- Eichel, M. A., Gargareta, V. I., D'Este, E., Fledrich, R., Kungl, T., Buscham, T. J., ... Werner, H. B. (2020). CMTM6 expressed on the adaxonal Schwann cell surface restricts axonal diameters in peripheral nerves. *Nature Communications*, *11*, 4514.
- Erwig, M. S., Patzig, J., Steyer, A. M., Dibaj, P., Heilmann, M., Heilmann, I., ... Werner, H. B. (2019). Anillin facilitates septin assembly to prevent pathological outfoldings of central nervous system myelin. *eLife*, *8*, e43888.
- Estey, M. P., Di Ciano-Oliveira, C., Froese, C. D., Bejide, M. T., & Trimble, W. S. (2010). Distinct roles of septins in cytokinesis: SEPT9 mediates midbody abscission. *The Journal of Cell Biology*, *191*, 741–749.
- Fabrizi, G. M., Taioli, F., Cavallaro, T., Rigatelli, F., Simonati, A., Mariani, G., ... Rizzuto, N. (2000). Focally folded myelin in Charcot-Marie-Tooth neuropathy type 1B with Ser49Leu in the myelin protein zero. *Acta Neuropathologica*, *100*, 299–304.
- Feltri, M. L., Poitelon, Y., & Previtali, S. C. (2016). How Schwann cells sort axons. *The Neuroscientist*, *22*, 252–265.
- Fledrich, R., Akkermann, D., Schütza, V., Abdelaal, T. A., Hermes, D., Schäffner, E., ... Stassart, R. M. (2019). NRG1 type I dependent autocrine stimulation of Schwann cells in onion bulbs of peripheral neuropathies. *Nature Communications*, *10*, 1467.
- Füchtbauer, A., Lassen, L. B., Jensen, A. B., Howard, J., de Quiroga, A. S., Warming, S., ... Füchtbauer, E.-M. (2011). Septin9 is involved in septin filament formation and cellular stability. *Biological Chemistry*, *392*, 769–777.
- Giese, K. P., Martini, R., Lemke, G., Soriano, P., & Schachner, M. (1992). Mouse PO gene disruption leads to hypomyelination, abnormal expression of recognition molecules, and degeneration of myelin and axons. *Cell*, *71*, 565–576.
- Gillespie, C. S., Sherman, D. L., Fleetwood-Walker, S. M., Cottrell, D. F., Tait, S., Garry, E. M., ... Brophy, P. J. (2000). Peripheral demyelination and neuropathic pain behavior in periaxin-deficient mice. *Neuron*, *26*, 523–531.
- Goebbels, S., Oltrogge, J. H., Wolfer, S., Wieser, G. L., Nientiedt, T., Pieper, A., ... Nave, K. A. (2012). Genetic disruption of Pten in a novel mouse model of tomaculous neuropathy. *EMBO Molecular Medicine*, *4*, 486–499.
- Golan, N., Kartvelishvily, E., Spiegel, I., Salomon, D., Sabanay, H., Rechav, K., ... Peles, E. (2013). Genetic deletion of Cadm4 results in myelin abnormalities resembling Charcot-Marie-Tooth neuropathy. *Journal of Neuroscience*, *33*, 10950–10961.
- Grosse, G. M., Bauer, C., Kopp, B., Schrader, C., & Osmanovic, A. (2020). Identification of a rare SEPT9 variant in a family with autosomal dominant Charcot-Marie-Tooth disease. *BMC Medical Genetics*, *21*, 45.
- Hamdan, H., Lim, B. C., Torii, T., Joshi, A., Konning, M., Smith, C., ... Rasband, M. N. (2020). Mapping axon initial segment structure and function by multiplexed proximity biotinylation. *Nature Communications*, *11*, 100.
- Hannibal, M. C., Ruzzo, E. K., Miller, L. R., Betz, B., Buchan, J. G., Knutzen, D. M., ... Chance, P. F. (2009). SEPT9 gene sequencing analysis reveals recurrent mutations in hereditary neuralgic amyotrophy. *Neurology*, *72*, 1755–1759.

- Hartline, D. K., & Colman, D. R. (2007). Rapid conduction and the evolution of giant axons and myelinated fibers. *Current Biology*, *17*, R29–R35.
- Hill, R. A., Li, A. M., & Grutzendler, J. (2018). Lifelong cortical myelin plasticity and age-related degeneration in the live mammalian brain. *Nature Neuroscience*, *21*, 683–695.
- Horn, M., Baumann, R., Pereira, J. A., Sidiropoulos, P. N. M., Somandin, C., Welzl, H., ... Suter, U. (2012). Myelin is dependent on the Charcot-Marie-Tooth type 4H disease culprit protein FRABIN/FGD4 in Schwann cells. *Brain*, *135*, 3567–3583.
- Huang, Y.-W., Yan, M., Collins, R. F., DiCiccio, J. E., Grinstein, S., & Trimble, W. S. (2008). Mammalian septins are required for phagosome formation. *Molecular Biology of the Cell*, *19*, 1717–1726.
- Iv, F., Martins, C. S., Castro-Linares, G., Taveneau, C., Barbier, P., Verdier-Pinard, P., ... Mavrikis, M. (2021). Insights into animal septins using recombinant human septin octamers with distinct SEPT9 isoforms. *Journal of Cell Science*, *134*, jcs258484.
- Jaegle, M., Ghazvini, M., Mandemakers, W., Piirsoo, M., Driegen, S., Levavasseur, F., ... Meijer, D. (2003). The POU proteins Brn-2 and Oct-6 share important functions in Schwann cell development. *Genes and Development*, *17*, 1380–1391.
- Jahn, O., Siems, S. B., Kusch, K., Hesse, D., Jung, R. B., Liepold, T., ... Werner, H. B. (2020). The CNS myelin proteome: Deep profile and persistence after post-mortem delay. *Frontiers in Cellular Neuroscience*, *14*, 239.
- Katanov, C., Novak, N., Vainshtein, A., Golani, O., Dupree, J. L., & Peles, E. (2020). N-wasp regulates oligodendrocyte myelination. *Journal of Neuroscience*, *40*, 6103–6111.
- Kim, M. S., Froese, C. D., Estey, M. P., & Trimble, W. S. (2011). SEPT9 occupies the terminal positions in septin octamers and mediates polymerization-dependent functions in abscission. *The Journal of Cell Biology*, *195*, 815–826.
- Kinoshita, M. (2003). Assembly of mammalian Septins. *Journal of Biochemistry*, *134*, 491–496.
- Kinoshita, M., Field, C. M., Coughlin, M. L., Straight, A. F., & Mitchison, T. J. (2002). Self- and Actin-templated assembly of mammalian septins. *Developmental Cell*, *3*, 791–802.
- Kuhlenbäumer, G., Hannibal, M. C., Nelis, E., Schirmacher, A., Verpoorten, N., Meuleman, J., ... Chance, P. F. (2005). Mutations in SEPT9 cause hereditary neuralgic amyotrophy. *Nature Genetics*, *37*, 1044–1046.
- Laccone, F., Hannibal, M. C., Neesen, J., Grisold, W., Chance, P. F., & Rehder, H. (2008). Dysmorphic syndrome of hereditary neuralgic amyotrophy associated with a SEPT9 gene mutation—A family study. *Clinical Genetics*, *74*, 279–283.
- Landsverk, M. L., Ruzzo, E. K., Mefford, H. C., Buysse, K., Buchan, J. G., Eichler, E. E., ... Hannibal, M. C. (2009). Duplication within the SEPT9 gene associated with a founder effect in North American families with hereditary neuralgic amyotrophy. *Human Molecular Genetics*, *18*, 1200–1208.
- Lappe-Siefke, C., Goebbels, S., Gravel, M., Nicksch, E., Lee, J., Braun, P. E., ... Nave, K.-A. (2003). Disruption of *Cnp1* uncouples oligodendroglial functions in axonal support and myelination. *Nature Genetics*, *33*, 366–374.
- Martini, R., Mohajeri, M. H., Kasper, S., Giese, K. P., & Schachner, M. (1995). Mice doubly deficient in the genes for PO and myelin basic protein show that both proteins contribute to the formation of the major dense line in peripheral nerve myelin. *Journal of Neuroscience*, *15*, 4488–4495.
- Martini, R., & Schachner, M. (1997). Molecular bases of myelin formation as revealed by investigations on mice deficient in glial cell surface molecules. *Glia*, *19*, 298–310.
- McDade, S. S., Hall, P. A., & Russell, S. E. H. (2007). Translational control of SEPT9 isoforms is perturbed in disease. *Human Molecular Genetics*, *16*, 742–752.
- McIlhatton, M. A., Burrows, J. F., Donaghy, P. G., Chanduloy, S., Johnston, P. G., & Russell, S. E. H. (2001). Genomic organization, complex splicing pattern and expression of a human septin gene on chromosome 17q25.3. *Oncogene*, *20*, 5930–5939.
- Mendonça, D. C., Macedo, J. N., Guimarães, S. L., Barroso da Silva, F. L., Cassago, A., Garratt, R. C., ... Araujo, A. P. U. (2019). A revised order of subunits in mammalian septin complexes. *Cytoskeleton*, *76*, 457–466.
- Mikoshiba, K., Kohsaka, S., Takamatsu, K., & Tsukada, Y. (1981). Neurochemical and morphological studies on the myelin of peripheral nervous system from Shiverer mutant mice: Absence of basic proteins common to central nervous system. *Brain Research*, *204*, 455–460.
- Möbius, W., Patzig, J., Nave, K. A., & Werner, H. B. (2008). Phylogeny of proteolipid proteins: Divergence, constraints, and the evolution of novel functions in myelination and neuroprotection. *Neuron Glia Biology*, *4*, 111–127.
- Musse, A. A., Gao, W., Homchaudhuri, L., Boggs, J. M., & Harauz, G. (2008). Myelin basic protein as a “PI(4,5)P2-modulin”: A new biological function for a major central nervous system protein. *Biochemistry*, *47*, 10372–10382.
- Nave, K.-A., & Werner, H. B. (2014). Myelination of the nervous system: Mechanisms and functions. *Annual Review of Cell and Developmental Biology*, *30*, 503–533.
- Nave, K.-A., & Werner, H. B. (2021). Ensheathment and myelination of axons: Evolution of glial functions. *Annual Review of Neuroscience*, *44*, 197–219.
- Nawaz, S., Kippert, A., Saab, A. S., Werner, H. B., Lang, T., Nave, K. A., & Simons, M. (2009). Phosphatidylinositol 4,5-bisphosphate-dependent interaction of myelin basic protein with the plasma membrane in oligodendroglial cells and its rapid perturbation by elevated calcium. *Journal of Neuroscience*, *29*, 4794–4807.
- Nawaz, S., Schweitzer, J., Jahn, O., & Werner, H. B. (2013). Molecular evolution of myelin basic protein, an abundant structural myelin component. *Glia*, *61*, 1364–1377.
- Neubauer, K., Boeckelmann, D., Koehler, U., Kracht, J., Kirschner, J., Pendiżwiat, M., & Zieger, B. (2019). Hereditary neuralgic amyotrophy in childhood caused by duplication within the SEPT9 gene: A family study. *Cytoskeleton*, *76*, 131–136.
- Ogawa, Y., & Rasband, M. N. (2009). Proteomic analysis of optic nerve lipid rafts reveals new paranodal proteins. *Journal of Neuroscience Research*, *87*, 3502–3510.
- Pantera, H., Shy, M. E., & Svaren, J. (2020). Regulating PMP22 expression as a dosage sensitive neuropathy gene. *Brain Research*, *1726*, 146491.
- Patzig, J., Erwig, M. S., Tenzer, S., Kusch, K., Dibaj, P., Möbius, W., ... Werner, H. B. (2016). Septin/anillin filaments scaffold central nervous system myelin to accelerate nerve conduction. *eLife*, *5*, e17119.
- Patzig, J., Jahn, O., Tenzer, S., Wichert, S. P., de Monasterio-Schrader, P., Rosfa, S., ... Werner, H. B. (2011). Quantitative and integrative proteome analysis of peripheral nerve myelin identifies novel myelin proteins and candidate neuropathy loci. *Journal of Neuroscience*, *31*, 16369–16386.
- Patzig, J., Kusch, K., Fledrich, R., Eichel, M. A., Lüders, K. A., Möbius, W., ... Werner, H. B. (2016). Proteolipid protein modulates preservation of peripheral axons and premature death when myelin protein zero is lacking. *Glia*, *64*, 155–174.
- Peterson, A. C., & Bray, G. M. (1984). Hypomyelination in the peripheral nervous system of shiverer mice and in shiverer in equilibrium normal chimaera. *The Journal of Comparative Neurology*, *227*, 348–356.
- Previtali, S. C. (2021). Peripheral nerve development and the pathogenesis of peripheral neuropathy: The sorting point. *Neurotherapeutics*, *18*, 2156–2168.
- Roth, A. D., Ivanova, A., & Colman, D. R. (2006). New observations on the compact myelin proteome. *Neuron Glia Biology*, *2*, 15–21.
- Roth, A. D., Liazoghli, D., Perez De Arce, F., & Colman, D. R. (2013). Septin 7: Actin cross-organization is required for axonal association of Schwann cells. *Biological Research*, *46*, 243–249.

- Schardt, A., Brinkmann, B. G., Mitkovski, M., Sereda, M. W., Werner, H. B., & Nave, K.-A. (2009). The SNARE protein SNAP-29 interacts with the GTPase Rab3A: Implications for membrane trafficking in myelinating glia. *Journal of Neuroscience Research*, *87*, 3465–3479.
- Sellin, M. E., Sandblad, L., Stenmark, S., & Gullberg, M. (2011). Deciphering the rules governing assembly order of mammalian septin complexes. *Molecular Biology of the Cell*, *22*, 3152–3164.
- Sellin, M. E., Stenmark, S., & Gullberg, M. (2014). Cell type-specific expression of SEPT3-homology subgroup members controls the subunit number of heteromeric septin complexes. *Molecular Biology of the Cell*, *25*, 1594–1607.
- Shuman, B., & Momany, M. (2021). Septins from protists to people. *Frontiers in Cell and Development Biology*, *9*, 824850.
- Siems, S. B., Jahn, O., Eichel, M. A., Kannaiyan, N., Wu, L. M. N., Sherman, D. L., ... Werner, H. B. (2020). Proteome profile of peripheral myelin in healthy mice and in a neuropathy model. *eLife*, *9*, e51406.
- Snaidero, N., Möbius, W., Czopka, T., Hekking, L. H. P., Mathisen, C., Verkleij, D., ... Simons, M. (2014). Myelin membrane wrapping of CNS axons by PI(3,4,5)P3-dependent polarized growth at the inner tongue. *Cell*, *156*, 277–290.
- Soroor, F., Kim, M. S., Palander, O., Balachandran, Y., Collins, R. F., Benlekbir, S., ... Trimble, W. S. (2021). Revised subunit order of mammalian septin complexes explains their in vitro polymerization properties. *Molecular Biology of the Cell*, *32*, 289–300.
- Stendel, C., Roos, A., Deconinck, T., Pereira, J., Castagner, F., Niemann, A., ... Senderek, J. (2007). Peripheral nerve demyelination caused by a mutant rho GTPase guanine nucleotide exchange factor, FRA-BIN/FGD4. *The American Journal of Human Genetics*, *81*, 158–164.
- Sturrock, R. R. (1976). Changes in neuroglia and myelination in the white matter of aging mice. *Journals of Gerontology*, *31*, 513–522.
- Sudo, K., Ito, H., Iwamoto, I., Morishita, R., Asano, T., & Nagata, K. (2007). SEPT9 sequence alternations causing hereditary neuralgic amyotrophy are associated with altered interactions with SEPT4/SEPT11 and resistance to Rho/Rhotekin-signaling. *Human Mutation*, *28*, 1005–1013.
- Suresh, S., Wang, C., Nanekar, R., Kursula, P., & Edwardson, J. M. (2010). Myelin basic protein and myelin protein 2 act synergistically to cause stacking of lipid bilayers. *Biochemistry*, *49*, 3456–3463.
- Terada, N., Saitoh, Y., Kamijo, A., Yamauchi, J., Ohno, N., & Sakamoto, T. (2019). Structures and molecular composition of Schmidt-Lanterman incisures. *Advances in Experimental Medicine and Biology*, *1190*, 181–198.
- Tooley, A. J., Gilden, J., Jacobelli, J., Beemiller, P., Trimble, W. S., Kinoshita, M., & Krummel, M. F. (2009). Amoeboid T lymphocytes require the septin cytoskeleton for cortical integrity and persistent motility. *Nature Cell Biology*, *11*, 17–26.
- Werner, H. B., Krämer-Albers, E. M., Strenzke, N., Saher, G., Tenzer, S., Ohno-Iwashita, Y., ... Nave, K. A. (2013). A critical role for the cholesterol-associated proteolipids PLP and M6B in myelination of the central nervous system. *Glia*, *61*, 567–586.
- Woods, B. L., & Gladfelter, A. S. (2021). The state of the septin cytoskeleton from assembly to function. *Current Opinion in Cell Biology*, *68*, 105–112.
- Yin, X., Baek, R. C., Kirschner, D. A., Peterson, A., Fujii, Y., Nave, K. A., ... Trapp, B. D. (2006). Evolution of a neuroprotective function of central nervous system myelin. *Journal of Cell Biology*, *172*, 469–478.
- Yoshida, M., & Colman, D. R. (1996). Parallel evolution and coexpression of the proteolipid proteins and protein zero in vertebrate myelin. *Neuron*, *16*, 1115–1126.

How to cite this article: Martens, A.-K., Erwig, M., Patzig, J., Fledrich, R., Füchtbauer, E.-M., & Werner, H. B. (2023). Targeted inactivation of the *Septin2* and *Septin9* genes in myelinating Schwann cells of mice. *Cytoskeleton*, *80*(7-8), 290–302. <https://doi.org/10.1002/cm.21736>